Study of the Reaction $K^+ + p \rightarrow K^0 + \pi^+ + p$ at 1.14 GeV/c

E. BOLDT,* J. DUBOC, N. H. DUONG, P. EBERHARD, R. GEORGE,†
V. P. HENRI,† F. LEVY, J. POYEN, AND M. PRIPSTEIN,
Laboratoire de Physique Atomique et Moléculaire, Collège de France, Paris, France

AND

J. CRUSSARD AND A. TRAN
Departement Saturne, Centre d'Etudes Nucleaires, Saclay, Gif-sur-Yvette, France

(Received 17 July 1963)

We report here the study of the inelastic process $K^+p \rightarrow K^0\pi^+p$ at 1.14 GeV/c [E_{tot}(c.m.)=1.859 GeV]. The study was done using the Saclay 35-cm hydrogen bubble chamber and analyzing events having a V^0 two-prong topology in the chamber. The total cross section for the reaction is 4.6±0.3 mb. The reaction is dominated by the production of the N_{33}^* and K^* (888 MeV) resonances. The nonresonating background, if any, contributes less than 0.6 mb to the total cross section. No events were found with two pions in the final state. The cross section for N_{33}^* production is 3.6±0.5 mb. The K^* production cross section (apart from possible interference contributions) is 0.9±0.3 mb. Our measured value for the mass of the N_{33}^* resonance is 1212±8 MeV with a full width of 72±13 MeV. A systematic analysis of the production and decay properties of the N_{33}^* was made. The N_{33}^* is produced with a pronounced spin alignment. Our data are consistent with a complete alignment of $\pm\frac{1}{2}$ with respect to the production plane normal or with an alignment of $\pm\frac{3}{2}$ with respect to some direction in the production plane, the most probable direction being the direction of the incident K^+. No evidence is seen for the existence of the K^* (730 MeV) resonance.

I. INTRODUCTION

THE Saclay 35-cm hydrogen bubble chamber was exposed to a separated beam of K^+ mesons at the Saturne proton accelerator, the K^+ lab momentum being 1.14 GeV/c at the center of the chamber. We present here a study of the inelastic process[1]:

$$K^+ + p \rightarrow K^0 + \pi^+ + p. \quad (1)$$

Examples of this reaction were easily identified in the cases in which the K^0 decayed into two charged pions and appeared in the bubble chamber as a two-prong interaction associated with a V^0. Only events having this topology were considered in the study of reaction (1).

Our beam momentum corresponds to a total available energy in the center-of-mass of E_{tot} (c.m.)=1.859 GeV. As a reference for our discussion we give in Table I the thresholds for different processes which may occur as competing reactions to reaction (1) but which could not be distinguished from it by their topology.

The reactions (1), (1a), (1b), (1c), (2), (3), and (4) listed in Table I can occur in our case, while reactions (2a) and (2b) each have too high a threshold to be present. In addition, as seen from Table I, any π^+ or p contamination in the beam would give a negligible contribution to the type of events under consideration; that is, since the beam lab momentum is 1.14 GeV/c then the π^+ in the beam are barely at the threshold for producing V^0's via reaction (5), while the p in the beam are far below threshold for V^0 production from reaction (6). Thus, our investigation of the reaction $K^+ + p \rightarrow K^0 + \pi^+ + p$, by looking for the K^0-charged decay mode, is virtually free from ambiguities caused by contamination in the K^+ beam. Moreover, a precise kinematical analysis of reaction (1) is possible, because (a) all particles in this reaction are measured and (b) at this incident beam momentum the particles in the final state are produced with average lab momentum in the approximate range of 300–500 MeV/c which allows for good measurements.

II. SUMMARY OF EXPERIMENTAL OPERATION CONDITIONS

The K^+ beam[2] was designed around the Saturne 3-GeV proton accelerator at Saclay. It was a one-stage separated beam (6 m of separation at 45 kV/cm) which collected K^+ particles coming off at an angle of 18.5 deg from a Cu target (0.4 cm high×1.5 cm wide×8 cm long), located in a straight section of the accelerator. The momentum of the K^+ mesons in the bubble chamber was 1.14±0.027 GeV/c (rms spread). This was the designed value and was verified by an analysis of the $K_{\mu 2}$ decays for which the muon decayed at rest in the chamber. The beam gave a separated image, 0.5 cm high and 4 cm wide (full width at half-maximum), at a mass slit 20 m from the target and was then defocused in the vertical plane to provide a final image approximately 8 cm high and 4 cm wide (i.e., along the "dip" direction in the chamber) at the center of the 35-cm

* Present address: Physics Department, Rutgers University, New Brunswick, New Jersey.
† Present address: CERN, Division TC, Geneva, Switzerland.

[1] A summary of the results has been published elsewhere: J. Duboc, N. H. Duong, P. Eberhard, R. George, V. P. Henri, F. Levi, J. Poyen, M. Pripstein, J. Crussard, and A. Tran, Phys. Letters **6**, 233 (1963).

[2] D. Berley, J. Duboc, N. H. Duong, P. Eberhard, R. George, V. P. Henri, J. Poyen, J. F. Allard, C. Bohy, E. Boldt, L. Jauneau, G. Kayas, D. Morellet, and D. Vaguelsy, Nucl. Instr. Methods (to be published).

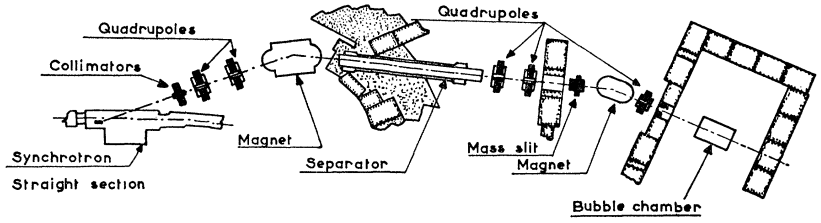

FIG. 1. Plan view of the experimental layout.

hydrogen bubble chamber, located 25 m from the target (see Fig. 1 for a sketch of the experimental layout). We had on the average 8 tracks per pulse in the chamber with between 1 and 2 K^+ per picture, under good operating conditions.

TABLE I. Possible and nearly possible reactions having a V^0-two-prong topology.

Reaction	Configuration in final state		Threshold total energy in c.m. system (in GeV)	Threshold lab momentum (in GeV/c)
$K^+p \to K^0p\pi^+$	nonresonating	(1)	1.576	
	$K^{*+}(730)+p$	(1a)	1.668	
	$N_{33}^{*+++}+K^0$	(1b)	1.736	
	$K^{*+}(888)+p$	(1c)	1.826	
$\to K^0p\pi^+\pi^0$	nonresonating	(2)	1.711	
	$N_{33}^{*+++}+K^{*0}(730)$	(2a)	1.968	
	$N_{33}^{*+++}+K^{*0}(888)$	(2b)	2.126	
$\to K^0n\pi^+\pi^+$		(3)	1.717	
$\to K^0p\pi^+\pi^0\pi^0$		(4)	1.846	
$\pi^+p \to \pi^+K^+\Lambda^0$		(5)		1.142
$pp \to K^+p\Lambda^0$		(6)		2.34

III. SELECTION OF EVENTS AND INTENSITY

In our scanning fiducial volume, we found 4188 K^+-one-prong decays with a projected angle ≥ 5 deg on one view, and 332 K^+-three-prong decays. The over-all scanning efficiency in that fiducial volume was found to be $\geq 99.5\%$. This number was obtained by scanning each picture twice by different scanners. The 5-deg cutoff for the K^+-one-prong decays was chosen partly for scanning efficiency reasons and partly because an elastic event would show a visible recoil proton if the scattering angle is ≥ 5 deg and would, therefore, be rejected. After correcting for angles <5 deg, using the accepted value for the ratio of $K\mu_2$ to $K\pi_2$ decays,[3] we found 5740 as the true number of one-prong K^+ decays in our fiducial volume. From this result we obtain the ratio of three-prong to one-prong K^+ decays as $332/5740 = 5.8 \pm 0.3\%$. This is in good agreement with the quoted value of 6%.[3]

In the same volume, we observed 240 V^0-two-prong interactions with the same scanning efficiency as listed above.

[3] Walter H. Barkas and Arthur H. Rosenfeld, Lawrence Radiation Laboratory Report UCRL-8030 Rev., 1961 (unpublished).

Among those events, we found the following categories:

(a) 13 events for which the measurement of the V^0-two-prong event was difficult, due to the malfunction of the optical system. (This malfunction did not, however, affect the number of the K^+ decay events counted.)

(b) 13 events had a distance between the two-prong apex and the V^0 vertex <1.5 mm.

(c) 5 events were actually "wrong" events in the sense that after kinematical fit of the V^0 it was found that the V^0 was nonassociated to the two-prong interaction or that the V^0 did not fit the K_1^0 hypothesis.

We removed the events in categories (a), (b), and (c) from the sample of 240 events and for the remaining 209 events we computed for each event the probability for the K_1^0 to be detected in the region between 1.5 mm from the apex and the limit of the fiducial volume. This gave us a statistical weight (i.e., the reciprocal of the detection probability) for each event which, when applied to the sample of 209 events and then correcting for the events in category (a), gives a true number of 265 V^0-two-prong events where the V^0 is an associated K_1^0. Then, from the lifetime of the K^+ mesons, $(1.224 \pm 0.013)\ 10^{-8}$ sec),[3] the momentum of the beam (1.14 GeV/c) and the ratio of the true V^0-two-prong events to the K^+ decays multiplied by a factor 3 to account for the other K^0 decay modes, we obtain the cross section for the K^0-two-prong events

$$\sigma = 4.6 \pm 0.3 \text{ mb}. \quad (7)$$

The quoted error includes the statistical errors on the true number of V^0-two-prong events and K^+ decay events, and the uncertainties in average beam momentum and the K^+ meson lifetime.

This value of the cross section is in agreement with our preliminary published results.[4]

IV. MEASUREMENT AND FITTING OF EVENTS

For purposes of investigating the properties of reaction (1) other than its cross section, we made an additional cutoff in the forward part of the fiducial volume, which reduced only slightly the number of V^0-two-prong events in the sample, from 209 to 206 events, but at the same time eliminated in an unbiased way those events having very large statistical weights—

[4] D. Berley, E. Boldt, J. Crussard, J. Duboc, P. Eberhard, R. George, V. P. Henri, F. Levy, and J. Poyen, Compt. Rend. Acad. Sci. **255**, 890 (1962).

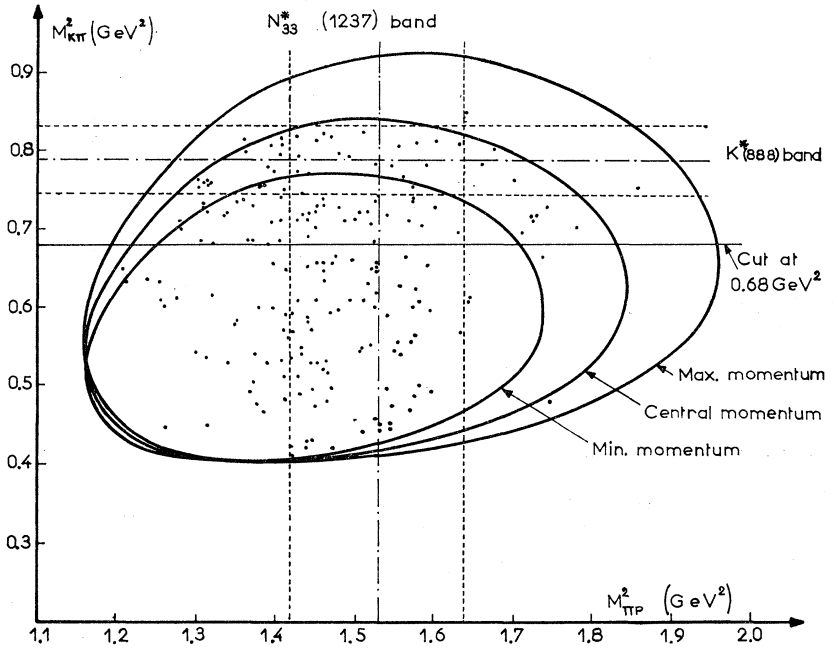

FIG. 2. Dalitz plot distribution. The dotted bands indicate the expected positions of the N_{33}^* and K^* (888 MeV) resonances.

thereby improving the precision of the experimental results; that is, the errors on the results obtained from the sample of 206 events tend to be smaller than those obtained from the original sample of 209 events, since the events with the largest weights have been eliminated.

A kinematic analysis of the 206 events was performed using the program GRIND,[5] on the Saclay IBM–7090 computer. A given hypothesis was rejected if its χ^2 value corresponded to a probability of less than 0.4%. All the events in the sample fitted the hypothesis (1) in Table I. Not a single event in the sample fitted the hypotheses (2) or (3); that is, we find no evidence of 2π production in our V^0-two-prong sample of K^+p inelastic scattering at this energy. (It is of interest to note that the same conclusion was found in K^-p inelastic scattering at the same beam energy.[6]) In addition, the effect of π^+ contamination in the beam was checked by testing hypothesis (5), $\pi^+p \rightarrow K^+\pi^+\Lambda^0$. None of the events in our sample fitted the latter hypothesis. Thus, the only remaining ambiguity in identifying completely the events was the ambiguity in associating the π^+ (hence the proton) with a specific prong in the case where the momenta of the two prongs were nearly equal. In this case, the kinematics program gave a good fit for reaction (1) when either one prong or the other was assumed to be the π^+ (or proton). Fortunately, this ambiguity in the track signature can be, and was, easily resolved by comparing the ionization densities of the two tracks, since the π^+ track was far less strongly ionizing than the proton track.

[5] GRIND 709 Kinematics Program Manual, CERN, Track Chamber Data Processing.
[6] W. Graziano and S. G. Wojcicki, Phys. Rev. **128**, 1868 (1962).

Thus, all the events in our sample were unambiguously identified as being of type (1) in Table I. Hence, the cross section quoted in the previous section, 4.6 $\pm$0.3 mb, which was based on the number V^0-two-prong events satisfying the scanning selection criteria and a kinematical fit of the V^0 only, really represents the measured cross section for the reaction $K^+p \rightarrow K^0\pi^+p$.

As a test of the existence of possible biases in the analysis, a check on parity conservation was performed. This was done as follows: Of the five four-momentum vectors describing the reaction, only four are independent because of energy-momentum conservation. Thus, if we consider any three of the five particles in the rest frame of a fourth particle, then the number of events in which the spatial vectors of the three particles form a right-handed system in that rest frame must equal the number in which they form a left-handed system, if parity is conserved. In our sample of 206 events, we find 115 events in which K^0, π^+, and outgoing p form a right-handed system in the lab and 91 events in which the same three particles form a left-handed one. Thus, within statistical errors, our result is consistent with parity conservation, indicating no apparent biases in our measurements.

V. DALITZ PLOT DISTRIBUTION

For each event in our sample of 206 events, the program GRIND calculated the square of the invariant mass of the πp and $K\pi$ systems (i.e., $M_{\pi p}{}^2$ and $M_{K\pi}{}^2$, respectively). The results are presented on the Dalitz plot in Fig. 2.

It should be remarked here that in this experiment the momentum spread (± 0.027 GeV/c) of the incident K^+ beam was not negligible and had to be taken into account for phase-space calculations. This was done in the following way. For ten different momenta within the K^+ beam momentum spread, the corresponding Dalitz "ellipses" (representing the locus of the kinematical limits in $M_{K\pi}^2$ and $M_{\pi p}^2$ for each momentum) were calculated. For purposes of clarity, we show in Fig. 2 only those "ellipses" corresponding to the minimum, central, and maximum beam momentum, respectively. The phase-space distribution ϕ, as a function of one of the parameters, for example $M_{\pi p}^2$, was then calculated by a numerical integration over the Dalitz plot of the expression $\phi(M_{\pi p}^2) = \int F(M_{K\pi}^2, M_{\pi p}^2) \times dM_{K\pi}^2$, where the integrand $F(M_{K\pi}^2, M_{\pi p}^2)$ is a weighting factor for each element of area on the Dalitz plot and is just equal to the percentage of the incident beam particles for which this element of area is available; for example, the area within the ellipse drawn for the minimum momentum is available to all incident beam particles so that $F(M_{K\pi}^2, M_{\pi p}^2) = 1$ for each element of area in this region, whereas each element along the boundary of the ellipse drawn for the central momentum is available to only 50% of the beam particles so that $F(M_{K\pi}^2, M_{\pi p}^2) = 0.5$ here.

For purposes of reference, the expected positions (i.e., published values)[7] of the $(T=\frac{3}{2}, J=\frac{3}{2})N_{33}^*$ resonance and $(T=\frac{1}{2}, J=1)K^*$ (888 MeV) resonance are indicated on the Dalitz plot by bands of dotted lines on the $M_{\pi p}^2$ and $M_{K\pi}^2$ axes, respectively. From the plot it is seen that there is a large region where the N_{33}^* and K^* bands overlap. For each event which occurs in this overlap region no distinction can be made as to which resonance it represents. In order to study the properties of the resonance, we follow the method of Eberhard and Pripstein[8] which overcomes the difficulty of having events with ambiguous signature (i.e., K^* or N_{33}^* signature) in the sample. This method can be summarized as follows.

For purposes of studying the N_{33}^* resonance, we ignore all events on the Dalitz plot having $M_{K\pi}^2 > 0.68$ GeV^2; that is, we ignore all events lying in the K^* band, including the events in the overlap region; in addition, by choosing the cutoff value in $M_{K\pi}^2$ sufficiently low, we ignore also those events lying outside the K^* band likely to be affected by interference effects between the K^* and N_{33}^* amplitudes. The remaining events in the sample then represent N_{33}^* events, nonresonating background, and events caused by interference between N_{33}^* and background. A test for the presence of the K^* (730 MeV) resonance, to be described in Sec. VI. C1, indicates that events of this type were not produced in our sample. From this sample then, the

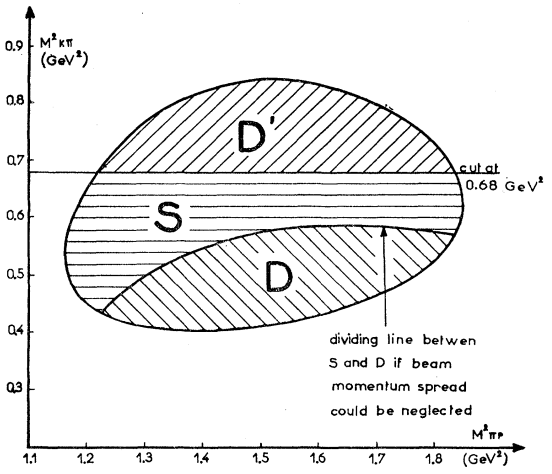

FIG. 3. Dalitz "ellipse" for the central beam momentum showing the approximate location of the S, D, and D' events for that particular beam momentum. The boundary between all the S and D events on the Dalitz plot can be described by a single line only in the case where the beam momentum spread is very small.

production and decay properties of the N_{33}^*, free from the effects of the K^*, can be determined if the method given in Ref. 8 is valid. The validity of the method was confirmed by various tests described in Appendix I. For each event in this sample, a spatial parity operation was performed on the $\pi^+ p$ system by interchanging the directions of the π^+ and proton in their own center of mass (c.m. system). This parity operation does not affect $M_{\pi p}^2$ but does change $M_{K\pi}^2$. We call the resulting event after the parity operation the conjugate of the original event. For each event on the Dalitz plot included in our sample (i.e., events with $M_{K\pi}^2 \leq 0.68$ GeV^2), we calculated the $M_{K\pi}^2$ of its conjugate event using the fitted value for the incident K^+ momentum in each case. The sample is then divided into two: subsample S with conjugate $M_{K\pi}^2 \leq 0.68$ GeV^2 and subsample D with conjugate $M_{K\pi}^2 > 0.68$ GeV^2. To illustrate, we show in Fig. 3 the approximate location of these sub-samples within the Dalitz "ellipse" corresponding to the central beam momentum only. When the whole momentum spread of the beam is taken into account then the boundary between all the S and D events can no longer be simply described by a single line.

Next, we corrected for the ignored events having $M_{K\pi}^2 > 0.68$ GeV^2 by repopulating this region of the Dalitz plot with the conjugate events of the true events in sample D. Then these fictitious conjugate events (denoted as sample D' in Fig. 3) represent a statistical sample of N_{33}^* and background events in this region, as if the coupling constant of producing the K^* resonance were turned off. Thus, the properties of the N_{33}^* and the background, free from the effects of the K^*, can be determined in an unbiased way from a study of the sample of $S+D+D'$.

To account for the fact that the subsample of

[7] Matts Roos, Rev. Mod. Phys. **25**, 314 (1963).
[8] Philippe Eberhard and Morris Pripstein, Phys. Rev. Letters **10**, 351 (1963).

fictitious conjugate events, D', is highly correlated statistically to subsample D, we consider the plot distributions of the events with respect to only those quantities which do not change sign under the restricted parity operation described above and use as our sample of events, N, where N is defined by the relation $N=S+2D$; that is, the sample N consists of S events and D events but with the statistical weight of the latter events doubled. The quantities unaffected by the restricted parity operation in the π^+p rest frame are $M_{\pi p}{}^2$, the production angle of the π^+p system (since it can be defined in terms of the K^+ and K^0 vectors in the over-all c.m. system) and the absolute value of the direction cosines of the π^+ with respect to any coordinate system in the π^+p rest frame.

Finally, the properties of the K^* and possible interference between $N_{33}{}^*$ and K^* can be determined from the experimentally obtained events having $M_{K\pi}{}^2>0.68$ GeV^2 (i.e., the previously ignored sample) and the D' events with their weights multiplied by the factor -1. We shall refer to this sample as the K sample (see Sec. VI. B).

VI. RESULTS

A. Analysis of the $N_{33}{}^*$ Resonance

1. *Mass Distribution and Intensity*

Figure 4 shows the mass distribution in the πp system for the sample of events, N. This histogram represents the mass spectrum of $N_{33}{}^*$ and background events only. We assumed that the $N_{33}{}^*$ distribution has a Breit-Wigner form and fitted the data in Fig. 4 with an expression of the form,

$$d\sigma/dM_{\pi p}{}^2=a_b|f_b(M_{\pi p}{}^2)|^2+2a_{bN^*}\,\mathrm{Re}\{f_b{}^*f_{N^*}\}+a_{N^*}|f_{N^*}(M_{\pi p}{}^2)|^2, \quad (8a)$$

where

$$|f_b(M_{\pi p}{}^2)|^2=k_b\phi(M_{\pi p}{}^2),$$
$$|f_{N^*}(M_{\pi p}{}^2)|^2=k_{N^*}\phi(M_{\pi p}{}^2)\times|1/[(M_{\pi p}{}^2-M_{N^*}{}^2)-i\eta_{N^*}]|^2, \quad (8b)$$
$$\{f_b{}^*f_{N^*}\}=(k_bk_{N^*})^{1/2}\phi(M_{\pi p}{}^2)\times 1/[(M_{\pi p}{}^2-M_{N^*}{}^2)-i\eta_{N^*}],$$

and where a_b=intensity of background production, a_{bN^*}=interference between background and $N_{33}{}^*$ amplitudes, a_{N^*}=intensity of $N_{33}{}^*$ production, $\phi(M_{\pi p}{}^2)$=3-body phase space for the $K^0\pi^+p$ final state (i.e., background) corrected for the beam momentum spread, k_b, k_{N^*}=normalization factors, M_{N^*}=mass of the $N_{33}{}^*$ in units of GeV, η_{N^*}=half-width at half-maximum for the $N_{33}{}^*$ resonance in units of GeV$^2=2M_{N^*}\Gamma_{N^*}/2$, Γ_{N^*}=total width of the $N_{33}{}^*$ resonance in units of GeV, and Re denotes the real part of the expression to its right.

From the definition of the terms in Eq. (8a), (8b) it is seen that we take into account the possibility of interference between background and $N_{33}{}^*$ amplitudes; however, we do not consider an interference term such as $2a_{bN^*}{}'(k_bk_{N^*})^{1/2}\phi(M_{\pi p}{}^2)\,\mathrm{Im}\{[(M_{\pi p}{}^2-M_{N^*}{}^2)-i\eta]^{-1}\}$ because such a term is of the same form as the term $a_{N^*}|f_{N^*}|^2$ and, hence, cannot be distinguished from it when making the fit. Also, it should be remarked that the existence of the interference term in Eq. (8) is not excluded by the test described in Appendix I, since the latter test is sensitive only to interference effects between the $N_{33}{}^*$ and a particular type of background.

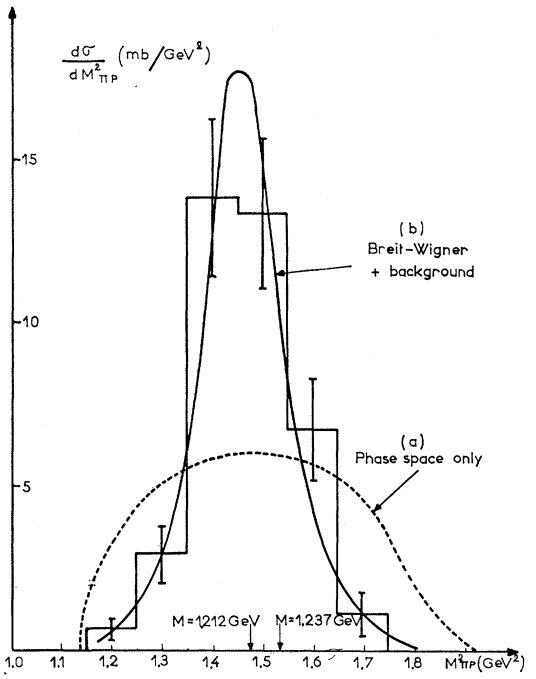

FIG. 4. Mass distribution of the π^+p system for sample N events. The curves represent the best fit for the hypotheses: (a) phase-space distribution only, and (b) background $+N_{33}{}^*$ of Breit-Wigner form+interference, as per Eq. (8a). Note that the areas of the curves (a) and (b) are not equal to the area of the histogram.

The normalization constants k_b and k_{N^*} were so chosen as to satisfy the normalization conditions,

$$\int|f_b(M_{\pi p}{}^2)|^2dM_{\pi p}{}^2=1=\int|f_{N^*}(M_{\pi p}{}^2)|^2dM_{\pi p}{}^2, \quad (9)$$

where the integration is taken over the entire Dalitz plot. Then the intensities a_b, a_{bN^*}, and a_{N^*} are expressed in units of mb. The interference intensity term, a_{bN^*}, has the property that its maximum value would be equal to $(a_ba_{N^*})^{1/2}$ (corresponding to a zero phase between the complex amplitudes of the background and of the $N_{33}{}^*$).

In addition to making a fit to the data in Fig. 4 with Eq. (8a), we have also attempted to fit the hypotheses: (A) that the data represent a phase space distribution only, and (B) that the data represent $N_{33}{}^*$ production only. The fits of these two hypotheses were

TABLE II. Fit of the $\pi^+ - p$ mass spectrum in Fig. 4 for various hypotheses.

Parameter \ Hypothesis	A Presence of phase-space background only	B Presence of N_{33}^* only	C Presence of background + N_{33}^* + interference, as per Eq. (8a)
$a_b + a_{N^*}$	3.1±0.3 mb[a]	3.6± 0.5 mb	3.6 ± 0.5 mb
a_b	3.1±0.3 mb[a]	0	−0.4 ± 0.3 mb
a_{bN^*}	0	0	−0.05± 0.1 mb
a_{N^*}	0	3.6± 0.5 mb	4.0 ± 0.7 mb
M_{N^*}	1237 MeV	1210 ± 5 MeV	1212 ± 8 MeV
Γ_{N^*}	90 MeV	62 ±10 MeV	72 ±13 MeV
Degrees of freedom	a_{N^*}	a_b, a_{bN^*}	none
χ^2 versus expected χ^2	83/1	2.6/2	···
Probability	0	30%	···
Over-all χ^2 versus expected χ^2	127/29	35/27	35/25

[a] When making a best-fit to a weighted sample of data, the normalization may depend upon the hypothesis tested. Therefore, the normalization for hypothesis (A) differs slightly from that for (B) and (C).

made with the technique described in Appendix II and the results are shown in Table II. The parameters listed are defined in Eq. (8). Where no error is quoted for the value of the parameter it implies that the value of the parameter is stipulated in the hypothesis. The χ^2 for the fit of Eq. (8) to the data cannot be computed with the technique described in Appendix II; instead the *over-all* χ^2 for this hypothesis was determined.

The results in Table II indicate very definitely the presence of the N_{33}^* resonance in our data. In fact, our data are consistent with the hypothesis of the presence of the N_{33}^* resonance, described by a Breit-Wigner shape weighted with phase space, and no contribution from background and interference terms. We consider as fitted values of the parameters those values determined from the fit of the most general hypothesis—that is, the fit of Eq. (8). The curve corresponding to the best-fit of this hypothesis is shown on Fig. 4. The fact that a_b is slightly negative just implies that the fitted curve has a smaller contribution at the tails of the distribution than for a pure Breit-Wigner form. The distribution is, however, positive everywhere (Fig. 4). In any case, the upper limit of the background contribution is ≤ 0.6 mb which is a two-standard-deviation limit from zero.

The most meaningful interpretation of the data is that of the presence only of the N_{33}^* described by a distribution similar to that of a Breit-Wigner but with smaller tails and whose cross section is given by $a_b + a_{N^*}$ in Table II. Thus, the total cross section for N_{33}^* production is 3.6±0.5 mb.

Our value for the mass of the N_{33}^*, $M_{N^*} = 1212 \pm 8$ MeV, is not in agreement with the published value (1237 MeV)[7] and is barely within two standard deviations from the mass (1225 MeV) corresponding to the position of the peak of the $\pi^+ p$ elastic scattering cross section curve.[9] Our value is, however, in excellent agreement with the value (1215 MeV) found by a Berkeley group[10] in studying the same inelastic reaction as ours at K^+ lab momentum of 1.96 GeV/c. The value for the width of the N_{33}^* resonance which we obtain, $\Gamma_{N^*} = 72 \pm 13$ MeV, is inconsistent with the value (145 MeV) tabulated by Gregory[11] but is consistent with the value (90±20 MeV) of Roos.[7,11a]

We have considered the possibility of biases in the measurements of $M_{\pi p}^2$, caused by using a wrong value for the bubble chamber magnetic field or a wrong beam momentum in making the kinematical fit of the data. An error of 5% in the magnetic field would affect M_{N^*} by 5 MeV and an error of 5% in beam momentum would change M_{N^*} by only 2 MeV. First, our measurements of the chamber magnetic field and beam momentum were far more accurate than to within 5% so that the error in these measurements would only introduce a negligible bias in the measurements of $M^2\pi p$. Secondly, we reran all events through the kinematics program GRIND, changing first the magnetic field by ±5% and then the beam momentum by ±5% from their original values, and found that many events no longer gave a kinematical fit for any of the V^0-two-prong hypotheses tested. For these two reasons then, it seems highly unlikely that the results obtained from the mass distributions are biased by wrong values for magnetic field and/or beam momentum.

2. *Angular Distributions*

To plot the various angular distributions of the N_{33}^*, we considered only those events in the sample N whose

[9] N. P. Klepikov, V. A. Meshcheryakov, and S. N. Sokolov, Joint Inst. for Nuclear Research Dubna–584 (1960).

[10] Sula Goldhaber, Talk Presented at the Athens Topical Conference on Recently Discovered Resonant States, 1963 (unpublished).

[11] B. P. Gregory, in *Proceedings of the 1962 International Conference on High-Energy Nuclear Physics at CERN* (CERN, Geneva, 1962), p. 783.

[11a] *Note added in proof.* Our value for the mass of the N_{33}^* is in good agreement with a prediction based on a ρ-photon analogy derived by L. Stodolsky and J. J. Sakurai [private communication to V.P.H.]. From this model one obtains [for E_{tot} (c.m.) = 1.859 GeV] a mass of 1211 MeV with a full width at half-maximum of 82 MeV. The shift from the canonical value of 1237 MeV is in part due to a momentum dependence term (p_f^3) where p_f is the momentum of the K^0 in the over-all c.m. system.

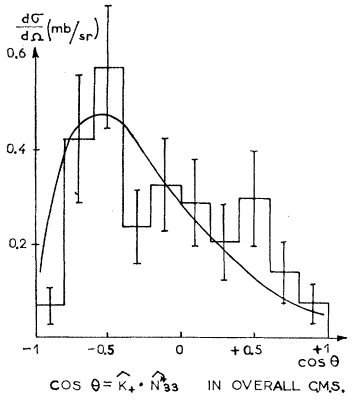

FIG. 5. Production angular distribution of the N_{33}^* in the K^+p c.m. system. The circumflex over a symbol in the definition of $\cos\theta$ denotes a unit momentum vector.

$M_{\pi p}$ values occur in the range 1160–1270 MeV in order to reduce even more the effect of background if any. This restricted sample corresponds to a cross section of 3.3 mb.

Figure 5 shows the production angular distribution of the N_{33}^* in the K^+p c.m. system, plotted as a function of $\cos\theta$ where θ is the angle between the incident K^+ and outgoing N_{33}^* in the K^+p c.m. system. The distribution indicates very little N_{33}^* production at $\theta=0$ and 180 deg, and a general peaking of N_{33}^* production in the backward hemisphere of the c.m. system—that is, a peaking for small momentum transfers. The curve shown in Fig. 5 is a theoretical computation by Jouvet *et al.*[12] for this production process, normalized to the cross section of our sample, 3.3 mb. This computation assumes that N_{33}^* production in K^+ inelastic charge-exchange scattering and in electron scattering involves the same intermediate states with the same relative amplitudes, apart from the presence of the photon in electron scattering. This curve is compatible with our data.

The decay angular distributions of the N_{33}^* in its own rest frame have been plotted with respect to the axes of three different rectangular coordinate systems α, β, and γ. The z axis is common to all three coordinate systems and is defined by the normal to the production plane. Specifically, the direction of the z axis is defined by the vector $(\hat{K}^+\times\hat{K}^0)$, where $\hat{K}^+$ and $\hat{K}^0$ are the three-momentum vectors of the K^+ and K^0 particles, respectively. The x axis of systems α, β, and γ is defined by the directions of the incident proton, outgoing K^0 and incident K^+, respectively, in the N_{33}^* rest frame. The y axis in each case is then perpendicular to the xz plane and lies in the production plane to form a right-handed system. The N_{33}^* decay angular distributions are shown in Fig. 6.

The distributions are plotted as functions of the absolute value of the direction cosines of the decay π in the coordinate systems α, β, and γ. Thus, $\cos\alpha_x$, $\cos\beta_x$, and $\cos\gamma_x$ are the direction cosines of the decay π with respect to the x axis and $\cos\alpha_y$, $\cos\beta_y$, and $\cos\gamma_y$ are the direction cosines with respect to the y axis, in the systems α, β, and γ, respectively [Fig. 6(a)]. The direction cosine with respect to the z axis (i.e., the production plane normal) is common to α, β, and γ and is denoted as $\cos\delta$ [Fig. 6(b)]. The histograms give a good indication of anisotropy in the decay of the N_{33}^* which implies a spin alignment for the N_{33}^* in the production process. This is discussed more fully in the next section.[12a]

It should be mentioned here that we have also measured an "Adair-type" angular distribution for the N_{33}^* decay with respect to that axis in the N_{33}^* rest frame along which the component of total angular momentum of the $K^0-N_{33}^*$ final state must be $\pm\frac{1}{2}$.[13] The resulting distributions for the decay π direction cosines in the coordinate system where this axis is taken as the x axis are almost identical to the ones in the coordinate system where the x axis is defined by the incident K^+ (Fig. 6). Thus any results and conclusions about the spin orientation of the N_{33}^* with respect to the K^+ direction are also valid for this "Adair-type" axis.

3. *Matrix of Alignment for the* N_{33}^*

A general and yet convenient description of the N_{33}^* decay with respect to any coordinate system in the N_{33}^* rest frame may be given in terms of its matrix of polarization, ρ (i.e., the density matrix of the decaying states), in that coordinate system. We consider the matrix of polarization in each of the coordinate systems α, β, and γ, defined in the preceding section, choosing the common z axis (i.e., the normal to the production plane) as the axis of quantization and assuming a total spin of $\frac{3}{2}$ for the N_{33}^* resonance. For this choice of axis of quantization, it can be shown that parity conservation in the production process imposes the condition that one half of all the terms in the matrix of polarization be equal to zero. Then for each of the coordinate systems, ρ has the general form,

$$\rho=\begin{pmatrix} \rho_{-3/2,-3/2} & 0 & \rho_{-3/2,+1/2} & 0 \\ 0 & \rho_{-1/2,-1/2} & 0 & \rho_{-1/2,+3/2} \\ \rho_{+1/2,-3/2} & 0 & \rho_{+1/2,+1/2} & 0 \\ 0 & \rho_{+3/2,-1/2} & 0 & \rho_{+3/2,+3/2} \end{pmatrix}, \quad (10)$$

[12] B. Jouvet, J. M. Abillon and G. Bordes, Phys. Letters **6**, 273 (1963).

[12a] *Note added in proof.* Our production angular distribution (Fig. 5) is also compatible with the recently published theory of L. Stodolsky and J. J. Sakurai [Phys. Rev. Letters **11**, 90 (1963)] and our decay angular distribution [Fig. 6(b)] is in very good agreement with a distribution of the form $1+3\cos^2\delta$ as predicted by the theory. We would like to point out that the best way to test for the hypothesis that the N_{33}^* production goes via an $M1$ transition is to test the hypothesis $Q=-1$, $R=I=0$, in our matrix of alignment description. [See Sec. VI. A3, Table IV, hyp. (4)α.]

[13] The "Adair-type" axis was defined from the four-momentum vector $\mathbf{V}=(E_p\mathbf{K}^+-E_{K^+}\mathbf{P})$, where E_p and E_{K^+} are the total energy of the incident proton and K^+ in the K^+p c.m. system, respectively, and where $\mathbf{P}$, $\mathbf{K}$ are the four-momenta of the incident proton and K^+, respectively. The "Adair-type" axis is taken as the spatial part of $\mathbf{V}$ in the N_{33}^* rest frame.

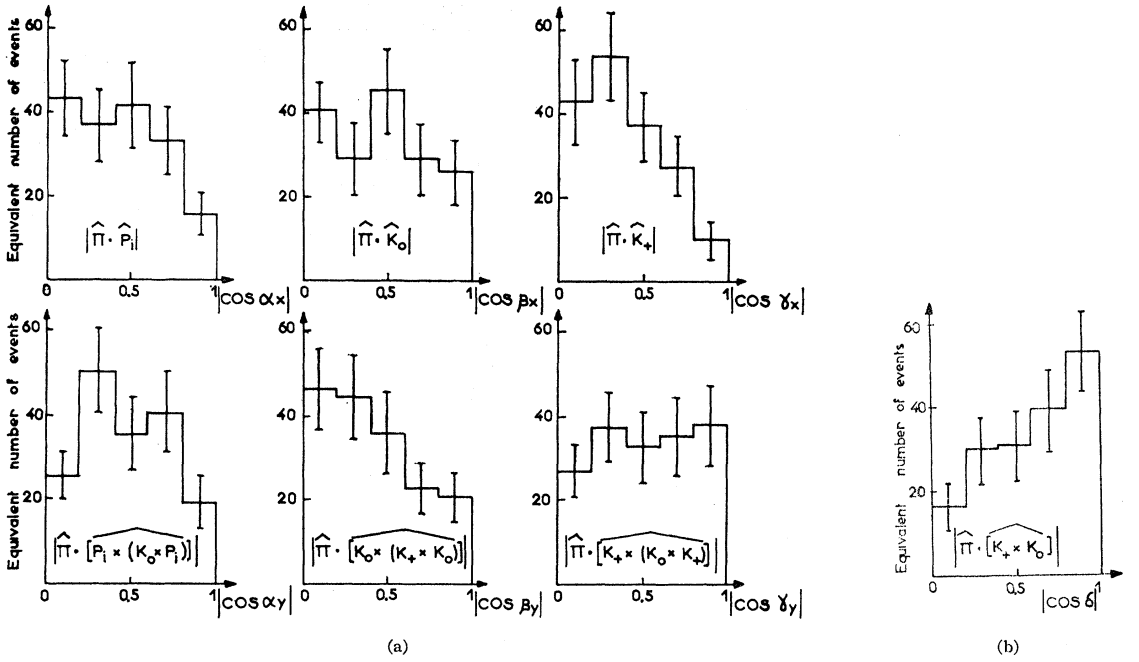

FIG. 6. Decay angular distributions of the N_{33}^* in its own rest frame. (a) Decay distributions with respect to various axes in the production plane; (b) decay distribution with respect to the production plane normal. The circumflex over a symbol in the definition of the various cosines denotes a unit momentum vector and all vectors are defined in N_{33}^* rest frame.

where the subscripts i and j of the matrix elements, ρ_{ij}, refer to the component of N_{33}^* spin along the axis of quantization. The matrix of polarization describes all the decay angular distributions of the N_{33}^* and the spin orientation of the decay proton in the particular coordinate system being considered. In our experiment we do not measure the decay proton spin; and therefore, we cannot measure all terms of the matrix of polarization ρ. However, we are able to measure an alignment of the N_{33}^* spin which can then be described by a matrix of alignment, A, defined by Eq. (11).

$$A_{ij}=\tfrac{1}{2}[\rho_{ij}+(-1)^{i-j}\rho_{ij}^*]. \tag{11}$$

This is equivalent to a definition of A in terms of the time-reversal operator, T; that is,

$$A=\tfrac{1}{2}[\rho+T\rho T^{-1}]. \tag{12}$$

Since for our choice of quantization axis the matrix elements are zero for $(i-j)$ being an odd integer, then for this case the matrix of alignment, A, is obtained by just averaging the terms symmetric with respect to the second diagonal of ρ.

We can express A in the form,

$$A=\tfrac{1}{4}\begin{pmatrix}(1+Q) & 0 & (R+iI) & 0\\ 0 & (1-Q) & 0 & (R+iI)\\ (R-iI) & 0 & (1-Q) & 0\\ 0 & (R-iI) & 0 & (1+Q)\end{pmatrix}, \tag{13}$$

where Q, R, and I are real numbers. The matrix A then describes completely the two-dimensional decay angular distribution in polar and azimuthal angles δ and φ. We determined the values of Q, R, and I from a fit to a two-dimensional histogram in δ and φ for the sample N events, where we considered only one hemisphere of the decay 4π-solid-angle sphere and transformed each event located in the other hemisphere into the first by a reflection about the center of the sphere. In such a distribution an event of the type D (Fig. 3) and its corresponding fictitious conjugate (type D') would be located in the same band of the histogram; therefore the sample N, where $N=S+2D$ (Sec. V), is a valid representation of the N_{33}^* events in such a distribution.

The best-fit values of Q, R, and I were calculated for coordinate systems α, β, and γ and the results are listed in Table III. In Table IV we list the χ^2 probabilities for various possible hypotheses of N_{33}^* spin orientation. From the results in Table IV we conclude that the N_{33}^* spin is definitely aligned. The spin component is either $\pm\frac{1}{2}$ with respect to the production plane normal or $\pm\frac{3}{2}$ with respect to some direction in the production

TABLE III. Best-fit values for the matrix of alignment parameters.

Coordinate system x axis defined by	α Incident proton	β Outgoing K^0	γ Incident K^+
Q	-0.77 ± 0.25	-0.84 ± 0.25	-0.77 ± 0.25
R	0.13 ± 0.20	-0.07 ± 0.20	0.54 ± 0.20
I	0.44 ± 0.25	-0.05 ± 0.25	0.02 ± 0.20

TABLE IV. χ^2-fits for various hypotheses of N_{33}^* spin orientation.

Hypothesis of N_{33}^* Spin orientation	Expected value of parameters Q	R	I	χ^2 probability in coordinate system with corresponding x axis: α Incident proton (%)	β Outgoing K^0 (%)	γ Incident K^+ (%)
(1) Zero alignment (i.e., isotropy in decay angular distribution)	0	0	0	0.05	1.2	0.02
(2) Complete alignment with spin component $\pm\frac{3}{2}$ with respect to the z axis	+1	0	0	0.06	0.6	0.05
(3) Complete alignment with spin component $\pm\frac{1}{2}$ in the production plane:						
(a) along x axis	+0.5	$-\frac{1}{2}\sqrt{3}$	0	<0.01	<0.01	<0.01
(b) along y axis	+0.5	$+\frac{1}{2}\sqrt{3}$	0	<0.01	<0.01	0.01
(4) Complete alignment with spin component $\pm\frac{1}{2}$ with respect to z axis	−1	0	0	17	90	7
(5) Complete alignment with spin component $\pm\frac{3}{2}$ in the production plane:						
(a) along x axis	−0.5	$+\frac{1}{2}\sqrt{3}$	0	4	0.2	35
(b) along y axis	−0.5	$-\frac{1}{2}\sqrt{3}$	0	0.07	3.5	0.02

plane. Of course the spin orientation may be described by a mixture of both alignments. The most probable direction for a complete alignment of $\pm\frac{3}{2}$ in the production plane is that of the incident K^+ (or the direction defined by the Adair-type axis discussed in Sec. VI. A2). Our data are inconsistent with zero alignment, alignment of $\pm\frac{3}{2}$ with respect to the production plane normal, an alignment of $\pm\frac{1}{2}$ in the production plane or with any mixture of the latter three alignments.

It should be pointed out that the decay angular distributions involve an integration over all the production angles. Therefore, if an alignment in the production plane is present, for instance along the K^+ direction (i.e., the x axis in the γ coordinate system), the integration over all the production angles may make this alignment appear in the β system as an alignment along the normal to the production plane—on the other hand, if the true alignment is along the z axis (common to all systems) the expected matrix of alignment is the same in all systems. For this reason then, in order to test against an alignment along the normal to the production plane, we have to look for the smallest χ^2 probability for this hypothesis in any of the coordinate systems.

B. Analysis of the K^* (888 MeV) Resonance

1. *Results from Sample K*

As described in Sec. V, the properties of the K^* and possible interferences between K^* and N_{33}^* can be determined from the sample of events K, consisting of the experimentally obtained events on the Dalitz plot having $M_{K\pi}^2>0.68$ GeV^2 (Fig. 2), plus the sample D' of fictitious conjugate events but with their weights multiplied by a factor -1. Fig. 7 shows the mass distribution of the $K^0-\pi^+$ system for this sample K. The existence of the K^* was tested by assuming a mass distribution of the Breit-Wigner form

$$a\{1/[(M_{K\pi}{}^2-M_{K^*}{}^2)^2+\eta_{K^*}{}^2]\},$$

with $M_{K^*}=888$ MeV, $\eta_{K^*}=2M_{K^*}\Gamma_{K^*}/2$, $\Gamma_{K^*}/2=25$ MeV,[7] and calculating the χ^2 probability for the hypothesis, $a=0$, to fit the data, using the method described in Appendix II. We obtained a $\chi^2=7.6$ for an

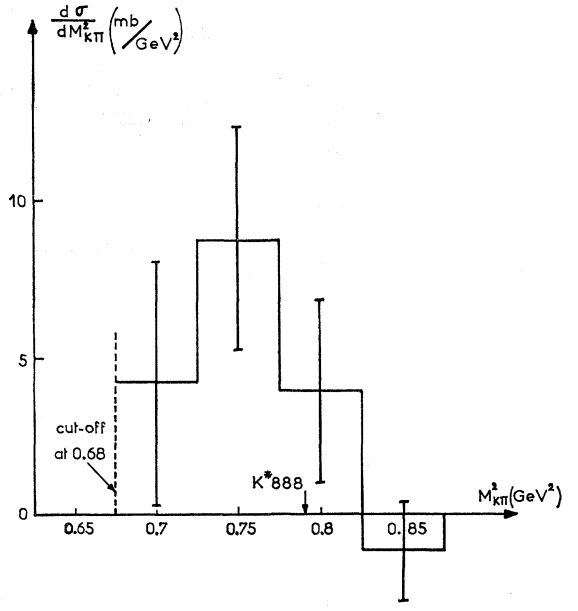

FIG. 7. Mass distribution of the $K^0\pi^+$ system for sample K events. The phase-space cutoff distorts the high $M_{K\pi}^2$ edge of the distribution causing a shift in the peak towards a smaller value of $M_{K\pi}^2$.

expected $\chi^2=1$, thereby ruling out this hypothesis. In other words, the existence of the K^* in the sample K data is established with odds of 1000/6.

To test the presence of interference effects between the K^* and N_{33}^*, we tested the symmetry of the decay angular distributions in the $K^0-\pi^+$ system, using only those events in sample K with $M_{K\pi}^2>0.70$ GeV^2. We computed $\langle\cos\theta\rangle_{\rm av}$, the average value of cosine of the π decay angle in the $K^0-\pi^+$ system, with respect to four directions in the plane of production, namely, with respect to the outgoing proton, the incident K^+ and the perpendicular to those particles. In each case the distribution should be symmetric (i.e., $\langle\cos\theta\rangle_{\rm av}=0$) if no interference was present. We find that the distributions deviated from symmetry by 2.0, 0.4, 0.025, and 3.0 standard deviations, respectively. Assuming that the distributions are uncorrelated, we calculate from these results a χ^2 of 12.6 for an expected χ^2 of 4, corresponding to a probability of 3% for the hypothesis of symmetry. If the distributions are actually correlated, then the 3.0 standard deviation result would make the symmetry hypothesis even more improbable. Thus, our data do provide an indication of interference between K^* and N_{33}^*, although the possibility of symmetry is not completely ruled out. The largest asymmetry is $\langle\cos\theta\rangle_{\rm av}=0.53\pm0.18$, where θ is the π decay angle in the $K^0-\pi^+$ rest frame with respect to the perpendicular to the K^+ direction in the production plane.

Because of the limited statistics in our sample of events and the apparent interference effect between the K^* and N_{33}^*, we cannot make any conclusions about the K^* production angular distribution or about the K^* spin alignment.

2. *A General Mass Distribution Fit*

We have made a fit of the two-dimensional mass distribution of all the true experimental data (Fig. 2), assuming a distribution of the form,

$$d^2\sigma/dM_{K\pi}{}^2dM_{\pi p}{}^2=a_b|f_b|^2+a_{N^*}|f_{N^*}|^2+a_{K^*}|f_{K^*}|^2 +2a_1\,\mathrm{Re}\{f_{N^*}{}^*f_{K^*}\}+2a_2\,\mathrm{Im}\{f_{N^*}{}^*f_{K^*}\}, \quad (13a)$$

where

$$|f_b|^2\propto\phi(M_{K\pi}{}^2,M_{\pi p}{}^2)=\text{phase space},$$
$$f_{N^*}\propto(\phi(M_{K\pi}{}^2,M_{\pi p}{}^2))^{1/2}/[(M_{\pi p}{}^2-M_{N^*}{}^2)-i\eta_{N^*}],$$
$$f_{K^*}\propto(\phi(M_{K\pi}{}^2,M_{\pi p}{}^2))^{1/2}/[(M_{K\pi}{}^2-M_{K^*}{}^2)-i\eta_{K^*}], \quad (13b)$$

and where $M_{N^*}=1212$ MeV, mass of the N_{33}^* (Sec. VI. A1), $\eta_{N^*}=2M_{N^*}\Gamma_{N^*}/2$, $\Gamma_{N^*}=72$ MeV, width of the N_{33}^* resonance (Sec. VI. A1), $M_{K^*}=888$ MeV, accepted value of K^* mass,[7] $\eta_{K^*}=2M_{K^*}\Gamma_{K^*}/2$, $\Gamma_{K^*}=50$ MeV, accepted value of the K^* width,[7] and a_b, a_{N^*}, a_{K^*}, a_1, a_2 are the intensities for background, N_{33}^* production, K^* production, and interference effects between K^* and N_{33}^*, respectively.

The terms $|f_b|^2$, $|f_{N^*}|^2$, and $|f_{K^*}|^2$ were each normalized to 1. No interference terms between N_{33}^* and background were included in Eq. (13a) because our previous tests (Sec. VI. A1) indicated that the contribution of such terms were negligible. The test of the hypothesis $a_{K^*}=a_1=a_2=0$, gave a χ^2 of 16 for an expected χ^2 of 3 (probability$=10^{-4}$). The test of the hypothesis that only $a_1=a_2=0$, gave a χ^2 of 3.3 for an expected χ^2 of 2. These results are further evidence of the presence of K^* in our data. We are consistent with no interference effects between K^* and N_{33}^* (because the errors are large and not because the fitted values are small). The best-fit for the parameters in Eq. (13) are listed in Table V. The cross sections for N_{33}^* and background production are consistent with the values obtained with the method in Sec. (VI. A1). Our value for the K^* production intensity is 0.9 ± 0.3 mb.

TABLE V. Results of the fit to the Dalitz plot mass distribution.

Parameter	Production products	Intensity (mb)
$a_b+a_{N^*}$	background+N_{33}^*	4.2 ± 0.5 mb
a_b	background	-0.5 ± 0.3 mb
a_{K^*}	K^*	0.9 ± 0.3 mb
a_1	interference, Re$\{K^*N^*\}$	$0.2+0.3$ mb
a_2	interference, Im$\{K^*N^*\}$	-0.7 ± 0.4 mb

C. Test for the Presence of Other Resonances

1. K^* (730 MeV) *Resonance*

We attempted a fit on the sample $S+D$ events (Fig. 3) in the Dalitz plot using a distribution of the form,

$$d^2\sigma/dM_{K\pi}{}^2dM_{\pi p}{}^2=a_b\begin{pmatrix}\text{phase}\\ \text{space}\end{pmatrix}+a_{N^*}\begin{pmatrix}\text{Breit-Wigner}\\ N^*\text{ distribution}\end{pmatrix} +a_{(730)}\begin{pmatrix}\text{Breit-Wigner}\\ K^*\text{ (730) distribution}\end{pmatrix}.$$

We tested the hypothesis $a_{(730)}=0$ and obtained a χ^2 of 0.7 for an expected $\chi^2=1$. Thus, our data are consistent with no presence of the K^* (730 MeV) resonance. In any case, the cross section for that resonance in our experiment would be <0.3 mb, which is a two-standard-deviation limit from 0 mb.

2. K^0-p *Resonance*

Because of the configuration of the N_{33}^* and K^* resonances on the Dalitz plot, it would be difficult to observe the presence of a K^0-p resonance unless it would be produced with a large cross section.

The K^0-p mass spectrum is fitted well by Eq. (13) with the values of the parameters listed in Table V, as shown in Fig. 8. Therefore, there is no need to postulate a K^0-p resonance to explain our data.

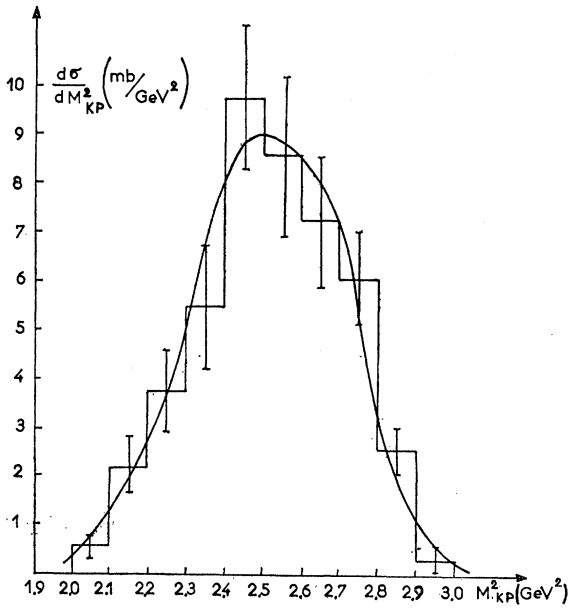

FIG. 8. Mass distribution of the K^0p system for all events on the Dalitz plot. The curve shown is defined by Eq. (13).

VII. CONCLUSIONS

From our study of the reaction $K^+p \to K^0\pi^+p$ at a total energy in the c.m. system of 1.859 GeV, we draw the following conclusions:

(1) The total cross section for the reaction is 4.6 $\pm$0.3 mb.

(2) The reaction is dominated by the N_{33}^* and K^* production modes. The nonresonating background, if any, contributes less than 0.6 mb to the total cross section. Moreover, no events were found with two pions in the final state. Because of insufficient energy in the c.m. system, such events for 2π production could occur only if no resonances were present in the final state.

(3) The cross section for N_{33}^* production is 3.6$\pm$0.5 mb and the K^* production cross section (apart from possible interference contributions) is 0.9$\pm$0.3 mb. The latter cross section is comparable to the cross section of 1.35$\pm$0.3 mb for $K^-p \to K^{*-}+p$ at the same energy.[6]

(4) Our measured value for the mass of the N_{33}^* resonance, 1212$\pm$8 MeV, is lower than the accepted value.[7,11]

(5) The width of the N_{33}^* resonance which we measure, 72$\pm$13 MeV, is smaller and inconsistent with the value listed in the CERN proceedings,[11] but is consistent with the value listed by Roos.[7]

(6) The production of the N_{33}^* is peaked in the backward hemisphere of the K^+p c.m. system (i.e., peaked for low-momentum transfer) with little or no N_{33}^* production in the extreme forward and backward directions. The N_{33}^* production angular distribution is consistent with the theoretical curve of Jouvet *et al.*[12]

(7) The N_{33}^* is produced with a pronounced spin alignment—our data are consistent with a complete alignment of $\pm\frac{1}{2}$ with respect to the production plane normal or with an alignment of $\pm\frac{3}{2}$ with respect to some direction in the production plane. We find the most probable direction for a complete alignment of $\pm\frac{3}{2}$ in the production plane to be the direction of the incident K^+ or the direction defined by the Adair-type axis (i.e., the axis in the N_{33}^* rest frame along which the component of total angular momentum of the $N_{33}^*+K^0$ final state is $\pm\frac{1}{2}$).

(8) Because of limited statistics and possible interference effects, we cannot draw any conclusions about the K^* spin alignment or about the production properties of the K^* other than its cross section.

(9) No evidence is seen for the existence of the K^* (730 MeV) resonance.

(10) There is no need to postulate the presence of a resonance in K^0-p system in the final state in order to explain our data.

ACKNOWLEDGMENTS

It is a pleasure to thank the many people who contributed in making this experiment a success. In particular, we thank Dr. R. Levy-Mandel and his team for the operation of the Saturne synchroton at Saclay, Professor A. Berthelot for the loan of the Saclay L.P.C.H.E. 35-cm hydrogen bubble chamber, MM. P. Prugne and A. Pacchioni and their crew for the good operation of the bubble chamber.

All this work could not have been done without the help of our scanners and technicians and we would like in particular to thank C. Calmels and P. Courty for their important contribution.

We wish to thank Miss G. Bordes and Dr. B. Jouvet for making their results available to us before publication.

Three of us (E. B., V. P. H., and M. P.) would like to thank the Commissariat à l'Energie Atomique for financial support during the experiment.

We would like to take this opportunity to thank Professor F. Perrin for his hospitality and for his support.

APPENDIX I: VALIDITY OF THE EVENT SAMPLES N AND K AS N_{33}^* RESONANCE AND K^* RESONANCE REPRESENTATIONS

The technique used to get a true representation of N_{33}^* and background properties (Secs. V and VI. A), as well as a true representation of K^* and interferences between K^* and N_{33}^* (Sec. VI. B1) is valid under the following assumptions:

(1) No important effect of the K^* (730 MeV). That effect, if it exists, must be small according to the tests made in Sec. VI. C1.

(2) No K^* contribution (even via interference effect) below the line of cut on the Dalitz plot, $M_{K\pi}{}^2=0.68$ GeV^2 (see Fig. 3). As a test, we compute the contribution in the region below that line of the term $a_{K^*}|f_{K^*}|^2$ and of both interference terms between N_{33}^* and K^*

defined in Eq. (13), using the fitted values shown in Table V. The a_{K^*} term gives a contribution of $+0.3$ mb and both interference terms give a contribution of -0.3 mb. These terms then should not distort the cross section for N_{33}^* [Eq. (8a)] but they may perturb slightly the measurement of the ratio of background to N_{33}^*. The effect then would be to make the a_b term even more negative.

(3) No large interference effect present between N_{33}^* and a background whose restricted parity, with respect to the operation of particle interchange for the π and proton in the $\pi-p$ system, would be opposite to the parity of N_{33}^*. This type of interference would cause an asymmetry in the decay angular distributions in the πp rest frame. We tested this symmetry of the angular distributions for the sample S by calculating $\langle\cos\theta\rangle_{\text{av}}$, the average value of the cos of the angle of the π in the $\pi-p$ rest frame with respect to four directions (i.e., incident proton, outgoing K^0, and their perpendiculars in the N_{33}^* production plane). The largest asymmetry was $\langle\cos\theta\rangle_{\text{av}}=0.1\pm0.1$—that is, within one standard deviation from the symmetry condition. Adding the results of the symmetry test with respect to the four directions mentioned, we obtain a χ^2 of 4.5 for an expected χ^2 of 4.

Thus, our tests indicate that none of the three effects listed above is present in our data which makes the technique used valid in our case.

APPENDIX II: DESCRIPTION OF THE TREATMENT OF STATISTICS USED

As we only use distributions of weighted events, the ordinate y_k in the band of any histogram always represents the sum of the weights of the events lying in that band k of the histogram. The error $\mathcal{E}_k$ is obtained by taking the square root of the sum of the square of the weights.

Although the histograms have been drawn with sufficiently large bands to remove most of the accidental peaks, the fits were always made with very small bands, since it can be shown that the errors in determining the parameters of the distributions are then minimized.

All tests were made assuming a finite number of free parameters, a_i, even when the number of bands was large. Then, a hypothesis was defined by stipulating the values of a restricted number of those parameters (denoted as type I parameters). We make a fit to the data letting all parameters free. The difference between the best-fit values and the values specified by the hypothesis for the type I parameters can be described by a vector $|\Delta|$ whose number of rows is equal to the number of type I parameters. We call W the corresponding error matrix for these parameters.

Then the χ^2 we refer to in the text, is given by the expression

$$\chi^2=|\tilde{\Delta}|W^{-1}|\Delta|\,,$$

where $|\tilde{\Delta}|$ is the transpose of $|\Delta|$. Thus, the type I parameters are just the degrees of freedom.

The above χ^2 is to be distinguished from the *over-all* χ^2 which refers to the standard χ^2 computed from the deviation between the experimental and fitted values of y_k and the corresponding values of $\mathcal{E}_k$ in each band of the histogram.